

Ab-initio Theory of Photoionization via Resonances

Adi Pick,^{1, a)} Petra Ruth Kaprálová-Žďánská,² and Nimrod Moiseyev^{1, b)}

¹⁾Faculty of Chemistry, Technion-Israel Institute of Technology, Haifa, Israel.

²⁾Department of Radiation and Chemical Physics, Institute of Physics, Academy of Sciences of the Czech Republic, Na Slovance 2, 182 21 Prague 8, Czech Republic

(Dated: 29 November 2023)

We present an *ab-initio* approach for computing the photoionization spectrum near autoionization resonances in multi-electron systems. While traditional (Hermitian) theories typically require computing the continuum states, which are difficult to obtain with high accuracy, our non-Hermitian approach requires only discrete bound and metastable states, which are accurately computed with advanced quantum chemistry tools. We derive a simple formula for the absorption lineshape near Fano resonances, which relates the asymmetry of the spectral peaks to the phase of the complex transition dipole moment. Additionally, we present a formula for the ionization spectrum of laser-driven targets and relate the “Autler-Townes” splitting of spectral lines to the existence of exceptional points in the Hamiltonian. We apply our formulas to compute the autoionization spectrum of helium, but our theory is also applicable for non-trivial multi-electron atoms and molecules.

We present an *ab-initio* approach for computing the photoionization spectrum near autoionization (AI) resonances in multi-electron systems. Recent developments in attosecond-laser technology enable probing and controlling photoionization processes, and lead to a renewed interest in ionization and related phenomena, such as high-harmonic generation and strong-field electronic dynamics^{1–5}. These experimental capabilities call for *ab-initio* theories, which can relate the electronic structure of the sampled medium to the measured ionization spectrum. However, most existing theories require the calculation of the continuum states^{6,7} (above the ionization threshold), which are difficult to obtain with high accuracy using standard quantum-chemistry numerical packages^{8,9}. In this work, we use non-Hermitian quantum mechanics (NHQM)¹⁰ in order to avoid the need of computing continuum states. Our theory produces an accurate and simple expression for the asymmetric ionization lineshape near autoionizing (AI) resonances, also called “Fano resonances”¹¹, [Eq. (7)] and a formula for the photoionization spectrum of laser-driven systems [Eq. (9)]. We relate the Autler-Townes¹² splitting of ionization spectral peaks to the existence of exceptional points¹³ (EPs), which are non-Hermitian degeneracies in which two AI states become degenerate and have the same energy and wavefunction. The full generality of our approach is revealed when evaluating our formulas with advanced non-Hermitian quantum-chemistry algorithms^{14,15}. Here, we demonstrate the predictions of our theory for helium using *ab-initio* electronic-structure data from Ref. 16,17.

In NHQM, the time-independent Schrödinger equation is solved with outgoing boundary conditions and the resulting energy spectrum is discrete, containing real-energy bound states and complex-energy metastable states¹⁰. This situation is very different from traditional Hermitian quantum mechanics (HQM), where metastable (autoionizing) states are described as real-energy solutions embedded in the ionization

continuum¹¹. Moreover, in HQM, the transition dipole moment is real, while in NHQM, it is generally complex. We show that the phase of the complex transition dipole moment has physical significance: it determines the asymmetry of the absorption peaks near AI states (see Fig. 1). Our derivation of the Fano asymmetry parameter is inspired by the recent work of Fukuta *et al.*¹⁸, which used a non-Hermitian approach to compute the Fano factor, although Ref. 18 introduced an artificial model for the continuum and did not relate the lineshape to the complex transition dipole moment.

As an application of our approach, we study the suppression and enhancement of autoionization in the presence of two lasers (a strong “pump” and a weak “probe”)—two effects which are similar in spirit to electromagnetically induced transparency (EIT) and absorption (EIA) [see Fig. 2]. Laser-induced suppression of photoionization was first measured in magnesium^{19,20}, and later demonstrated experimentally in several other systems (e.g., helium²¹ and sodium²²). These results were modeled using the Feshbach formalism^{20,23} and, therefore, require the computation of the continuum states, which can be avoided by our approach. Motivated by the huge impact of EIT in optics and atomic physics, we believe that the ability to accurately compute these effects for AI states will open new routes for controlling and understanding ionization and strong-field dynamics.

Let us begin by reviewing the traditional theory of optical absorption in autoionizing systems. Consider an atom or molecule in the presence of a weak linearly polarized electromagnetic field (with amplitude \mathcal{E} and polarization axis \hat{x}). In HQM, the absorption spectrum is calculated using Fermi’s golden rule²⁴

$$S(\omega) = \frac{|\mathcal{E}|^2}{\hbar} \sum_f |\langle \phi_i | x | \phi_f \rangle|^2 \delta(\hbar\omega - \varepsilon_f + \varepsilon_i). \quad (1)$$

Here, $\varepsilon_{i,f}$ and $|\phi_{i,f}\rangle$ are the initial- and final-state energies and wavefunctions respectively, while \sum_f denotes summation over bound and integration over continuum final states. Since continuum states have delocalized wavefunctions, it is a challenge to compute them with the same level of accuracy as the bound states in most existing quantum chemistry packages^{8,9}. This

^{a)} Also at Faculty of Electrical Engineering, Technion-Israel Institute of Technology, Haifa, Israel.; Electronic mail: adipick@gmail.com

^{b)} also at Faculty of Physics, Technion-Israel Institute of Technology, Haifa, Israel.

difficulty can be circumvented by using the Green's function eigenstate-free formula^{24,25}, which can be derived as follows. Using a mathematical identity for the δ -function²⁶, one can rewrite Eq. (1) as

$$S(\omega) = \sum_f \langle \phi_i | x | \phi_f \rangle \left(\frac{1}{\hbar\pi} \text{Im} \lim_{s \rightarrow 0^+} \frac{|\mathcal{E}|^2}{\hbar\omega - is - \varepsilon_f + \varepsilon_i} \right) \langle \phi_f | x | \phi_i \rangle. \quad (2)$$

Then, by using the normal-mode expansion of the excited states' Green's function²⁷, $G_{\text{exc}}(\varepsilon) \equiv \mathbb{X}_f |\phi_f\rangle \langle \phi_f| / (\varepsilon - \varepsilon_f)$, Eq. (2) takes the form

$$S(\omega) = \frac{|\mathcal{E}|^2}{\hbar\pi} \text{Im} \langle \phi_i | x G_{\text{exc}} x | \phi_i \rangle, \quad (3)$$

where $G_{\text{exc}}(\varepsilon)$ is evaluated at $\varepsilon = \hbar\omega + \varepsilon_i$.

Although Eq. (3) has clear advantages over Eq. (1), computing the full Green's function of multi-electron systems with traditional methods is still a very demanding computation. However, the Green's function formulation naturally extends to NHQM, which offers a huge computational advantage. Under the conditions stated below, one can simply replace the Hermitian normal-mode expansion of G_{exc} in Eq. (3) with the non-Hermitian quasi-normal modal expansion^{10,28}:

$$G_{\text{exc}}(\varepsilon) = \sum_f \frac{|\phi_f^R\rangle \langle \phi_f^L|}{(\phi_f^L | \phi_f^R)} \frac{1}{\varepsilon - \varepsilon_f}. \quad (4)$$

Here, $|\phi_f^R\rangle$ and ε_f are the discrete eigenvectors and eigenvalues of the (non-Hermitian) time-independent Schrödinger equation with outgoing boundary conditions, while $|\phi_f^L\rangle$ are the eigenvectors of the transposed equation. Round brackets denote the “unconjugated brackets:” $(\phi_i^L | \phi_f^R) \equiv \int dx \phi_i^L \phi_f^R dx^{10}$, which generalize the traditional Dirac brackets, $\langle \phi_i | \phi_j \rangle \equiv \int dx \phi_i^* \phi_j = \delta_{ij}^{29}$, for non-Hermitian Hamiltonians. The Hermitian and non-Hermitian modal expansions for G_{exc} agree when evaluated near resonant energies ($\varepsilon \approx \text{Re}[\varepsilon_f]$) and not too far away from the light–atom interaction region^{30,31}. Since we consider, in this work, resonant absorption and the absorption probability depends on overlap integrals between extended AI states and localized bound states, these conditions are satisfied for all cases of interest. However, when the Hamiltonian contains EPs, the modal expansion formula becomes invalid^{32–34}. The “unconjugated norm” $(\phi_i^L | \phi_f^R)$ vanishes at an EP and the associated term in Eq. (4) blows up. One can obtain a corrected formula for G_{exc} at the EP by considering Eq. (4) *near the EP* and carefully taking the limit of approaching the EP; one finds that two terms in the sum diverge with opposite signs, while their sum remains finite. This point was previously realized in the context of spontaneous emission near EPs in Ref. 28 [see supporting information (SI) for details].

By substituting Eq. (4) into Eq. (3), we obtain the NHQM absorption spectrum formula:

$$S(\omega) = \frac{|\mathcal{E}|^2}{\hbar\pi} \text{Im} \sum_f \frac{(\phi_i^L | x | \phi_f^R) (\phi_f^L | x | \phi_i^R)}{(\phi_f^L | \phi_f^R) (\hbar\omega - \varepsilon_f + \varepsilon_i)}. \quad (5)$$

This formula applies to cases where the initial state is bound and, therefore, one can replace Dirac bracket states, $|\phi_i\rangle$ and $\langle \phi_i|$, with unconjugated bracket states $|\phi_i^R\rangle$ and $\langle \phi_i^L|$ (since the left eigenvector of a Hermitian Hamiltonian is equal to the conjugated right eigenvector of the same eigenvalue). However, when the initial state is metastable, one needs to keep the conjugated bracket for the initial state. Our derivation of Eq. (5) is similar in spirit to the recent work of Fukuta *et al.*¹⁸, which used NHQM to compute the absorption spectrum. However, the latter work introduced an artificial model for the continuum, which is avoided in our approach.

Our new non-Hermitian formula [Eq. (5)] provides a simple interpretation for the asymmetric peaks near AI (Fano) resonances. The original Fano work¹¹ showed that the spectrum near an isolated resonance with frequency Ω and lifetime $1/\gamma$ can be written as

$$S_F(\omega) = S_0(\omega) \frac{(\omega - \Omega + \frac{\gamma}{2}q)^2}{(\omega - \Omega)^2 + (\frac{\gamma}{2})^2}, \quad (6)$$

where $S_0(\omega)$ is the background absorption due to continuum states and the remaining expression is the resonant peak. The parameter q determines the asymmetry of the resonant peak: the limit of $q \rightarrow \infty$ implies a Lorentzian, while $q \simeq 1$ yields an asymmetric lineshape. In traditional HQM, q is found by computing overlap integrals involving bound and continuum states^{11,26}. In our approach, however, the q factor depends on a single term in the sum in Eq. (5). By taking the ratio of the symmetric and anti-symmetric parts of that term, we obtain

$$q = \frac{\text{Re} \mu_{if}^2}{\text{Im} \mu_{if}^2} \left[1 \pm \sqrt{1 + \left(\frac{\text{Im} \mu_{if}^2}{\text{Re} \mu_{if}^2} \right)^2} \right], \quad (7)$$

where we introduced the shorthand notation $\mu_{if}^2 \equiv (\phi_i^L | x | \phi_f^R) (\phi_f^L | x | \phi_i^R)$. The sign of q indicates whether the absorption peak is blue or red shifted, and is determined by the sign of $\text{Im} \mu_{if}^2$. Our derivation of Eq. (7) generalizes the approach of Ref. 18. More details on the derivation are given in the SI.

As an example for application of Eq. (7), we compute the asymmetric absorption peaks near AI states in parahelium (i.e., helium atoms in which the spins of the two electrons are in the singlet state). The energy levels and dipole-allowed transitions are shown in Fig. 1(a). The states are labeled according to the approximate Hartree–Fock orbitals. All states below the ionization threshold are bound, while all double-excitation states are metastable AI states. We use data from Ref. 16,17 for the energy levels, lifetimes, and complex transition dipole moments. Figure 1(b) shows the ionization spectrum near three transitions in the XUV range, obtained by evaluating Eq. (5). The x -axis denotes the frequency offset between the field and the probed atomic transition. The plots demonstrate that our new formula for the Fano q factor [Eq. (7)] predicts the asymmetry of the lines, while the width of the peak is set by the imaginary part of the metastable-state energy.

Next, we turn to study photoautoionization in laser-driven atoms and molecules. Specifically, we consider cases where

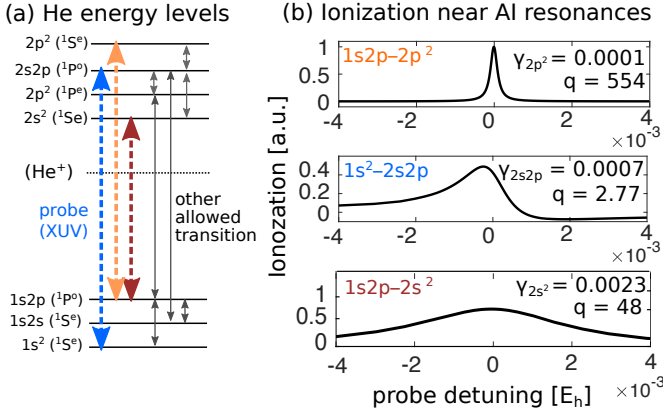


FIG. 1. (a) Energy levels of parahelium, including three bound states and four autoionization resonances [calculated in Ref. 17]. Thick dashed arrows mark the probed transitions, while narrow arrows mark additional dipole-allowed transitions. (b) Autoionization spectrum [evaluated using Eq. (5)] near the three probed transitions from (a) and the corresponding q asymmetry factor [evaluated using Eq. (7)]. The x -axis denotes the frequency offset between the field and the probed atomic transition.

a “pump laser” couples two (or more) AI states and a “probe laser” drives transitions from the ground to the AI states. A time-periodic probed system (denoted by H_0) has Floquet solutions the form³⁵:

$$\Psi_{\alpha,m}(x,t) = e^{-i\epsilon_{\alpha,m}t/\hbar} \Phi_{\alpha,m}(x,t). \quad (8)$$

Here, $\Phi_{\alpha,m}$ and $\epsilon_{\alpha,m}$ are the eigenvectors and eigenvalues of the Floquet Hamiltonian, $\mathcal{H} \equiv H_0 - i\hbar \frac{\partial}{\partial t}$. The quasienergies are frequency-periodic, $\epsilon_{\alpha,m} = \epsilon_{\alpha,0} + m\hbar\omega_0$, where ω_0 is the frequency of the probe, and the eigenvectors obey $\Phi_{\alpha,m}(t) = \Phi_{\alpha,0}(t)e^{i\omega_0 mt}$. The quantum number m is called the “Floquet channel.” In the SI, we use a generalized Fermi-Floquet golden rule³⁶ (which is valid for weak probe intensities) to derive a formula for the absorption spectrum of laser-driven systems. We obtain

$$S(\omega) = \frac{|\mathcal{E}|^2}{\hbar\pi} \text{Im} \sum_{f,m} \frac{((\Phi_{i,0}^L | x | \Phi_{f,m}^R))((\Phi_{f,m}^L | x | \Phi_{i,0}^R))}{\hbar\omega + m\hbar\omega_0 - \epsilon_{f,0} + \epsilon_{i,0}}. \quad (9)$$

Here $|\Phi_{i,0}\rangle$ and $|\Phi_{f,m}\rangle$ are the initial (bound) and final (metastable) Floquet states while $\epsilon_{i,0}$ and $\epsilon_{f,0}$ are the corresponding quasienergies in the zeroth Floquet channel. We use double brackets to denote spatial and temporal integration: $((\Phi_{\alpha,m}^L | \Phi_{\beta,n}^R)) \equiv \frac{1}{T} \int_0^T dt' \int_{-\infty}^{\infty} dx \Phi_{\alpha,m}^L(t',x) \Phi_{\beta,n}^R(t',x)$. In order to evaluate Eq. (9), it is convenient to expand the Floquet states, $|\Phi_{f,m}\rangle$, in the basis of eigenvectors of the field-free Hamiltonian (obtained by subtracting from H_0 the light-matter interaction term). In the SI, we review this standard procedure^{37,38} and present an explicit expression for the spectrum in terms of field-free eigenstates [Eq. (C22)].

Next, we apply Eq. (9) to compute the autoionization spectrum of laser-driven parahelium. As shown in Fig. 2(a), we consider an XUV probe, which drives the transition between the ground state [$1s^2(^1S)$] and the AI state $2s2p(^1P)$ and a

strong NIR pump, which resonantly couples two AI states. We consider two cases: (i) The pump couples the states $2s2p(^1P)$ and $2p^2(^1S)$ [green arrow in Fig. 2(a)] and (ii) The pump couples $2s^2(^1S)$ and $2s2p(^1P)$ (red arrow). The difference between the two cases is that in the former, the probe couples the ground state to the broader AI state (out of the two coupled AI states), while in the latter, the probe couples the ground state to the narrower AI state. It turns out that these two situations lead to drastically different ionization spectra. In the former case [shown in Fig. 2(b)], the effect of the pump is to suppress the ionization when the probe-photon energy is resonant with the atomic transition. The narrow dip in the autoionization spectrum is similar in spirit to the transparency window in EIT. As shown in the early work of Ref. 19, the suppression occurs due to coherent trapping of the atomic population in the ground state. In contrast, in the latter case [shown in Fig. 2(c)], the ionization lineshape is Lorentzian for weak pump amplitudes [similar to electromagnetically induced absorption (EIA)]. As the pump exceeds a critical value (denoted by $\mathcal{E}_0 = \mathcal{E}_{EP}$), the peak splits into two non-overlapping dressed-state peaks. At the splitting point, the Hamiltonian has an EP, as discussed below. Panels (b–c) show the splitting of the ionization peaks upon increasing the pump amplitude beyond the critical point (we show four pump values $\mathcal{E}_0/\mathcal{E}_{EP} = 1, 2, 6, 10$). Our *ab-initio* calculation takes into account all the dipole-allowed transitions in parahelium, although the atomic population predominantly occupies only three states in all cases under study.

When the pump amplitude significantly exceeds \mathcal{E}_{EP} (at $\mathcal{E} \approx 70\mathcal{E}_{EP}$), pairs of resonances merge again at ordinary de-

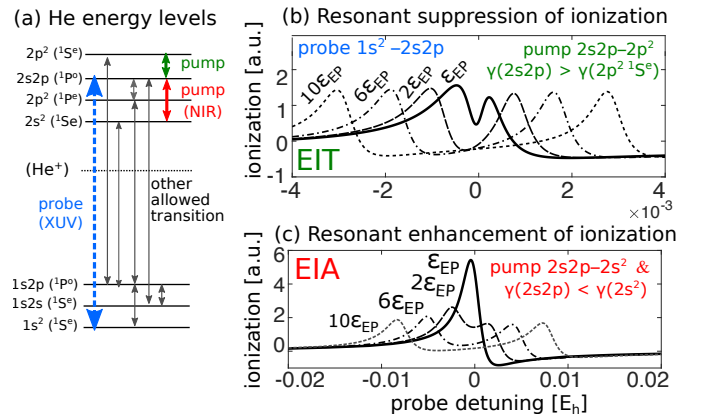


FIG. 2. (a) Energy levels of parahelium [as in Fig. 1]. The thick dashed (solid) arrow marks the probed (pumped) transitions, while narrow arrows mark additional dipole-allowed transitions. (b) Ionization spectrum of laser-driven helium [evaluated using Eq. (9)], when the probe couples the ground state to the wider resonance, demonstrating suppression of ionization when the probe is resonant with the atomic transition (similar to EIT). Four pump amplitudes are shown: $\mathcal{E}/\mathcal{E}_{EP} = 1, 2, 6, 10$. The x -axis denotes the frequency offset between the field and the probed atomic transition. (c) Similar to (b), but here the probe couples the ground state to the narrow AI state. In this case, the resulting spectrum is Lorentzian at weak pumps, and the lineshape resembles EIA.

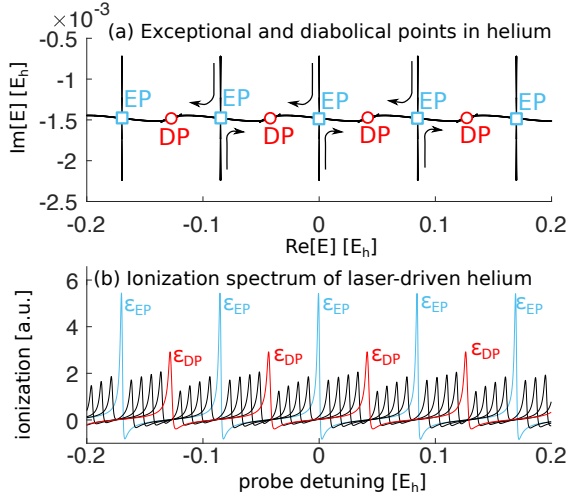


FIG. 3. (a) Trajectories of eigenvalues of the Floquet Hamiltonian upon changing the pump amplitude. Eigenvalues merge at exceptional and diaboloical points (EPs and DPs), marked by cyan triangles and red circles. (b) Relative absorption as a function of probe detuning for six pump amplitudes: $\mathcal{E}_0/\mathcal{E}_{EP} = 1, 11, 22, 33, 44, 55$. The peak absorption at EPs (cyan solid) is twice larger than DPs (red dashed). The x-axis denotes the frequency offset between the field and the probed atomic transition.

generacies, called diaboloical points (DPs). The trajectories of the complex eigenvalues of the Floquet Hamiltonian [see SI, Eqs. (C6,C7)] are shown in Fig. 3(a). Panel (b) shows the absorption spectrum at varying pump intensities for the case where the pump couples $2s^2(^1S)$ and $2s2p(^1P)$ [case (ii) above]. The plot demonstrates that the peak of the ionization spectrum near EPs is significantly larger than near the DPs (i.e., four-fold instead of two-fold), although the imaginary parts of the degenerate eigenvalues are approximately equal. This demonstrates the increased density of states at EPs (similar to the effect shown in spontaneous emission near EPs in Maxwell's equations²⁸).

In order to see that the point at which the spectral peaks split is an EP, we introduce a simplified model, where we keep only three electronic states (i.e., we keep only the ground state and a pair of AI state) and employ the rotating wave approximation (RWA) to eliminate rapidly rotating terms due to both the pump and the probe. By using the RWA, a three-level system can be described by the stationary effective Hamiltonian:

$$H = \begin{pmatrix} E_g + \hbar\omega_1 & -\frac{\mu_1\mathcal{E}_1}{2} & 0 \\ -\frac{\mu_1\mathcal{E}_1}{2} & E_1 - i\gamma_1 & -\frac{\mu_2\mathcal{E}_2}{2} \\ 0 & -\frac{\mu_2\mathcal{E}_2}{2} & E_2 - i\gamma_2 - \hbar\omega_2 \end{pmatrix} \quad (10)$$

Here, E_g is the ground-state energy, $E_{1,2}$ and $\gamma_{1,2}^{-1}$ are the excited-state energies and lifetimes and $\mu_{1,2}$ are the complex transition dipole moments of the allowed transitions. $\omega_{1,2}$ and $\mathcal{E}_{1,2}$ are the frequencies and amplitudes of the probe and pump fields respectively. The dashed lines in Eq. (10) mark the excited-state Hamiltonian, H_{exc} , whose complex eigenvalues

(ϵ_{\pm}) and eigenvectors (ϕ_{\pm}) coalesce at an EP when the pump frequency and amplitude are³⁹

$$\Delta_{EP} \equiv \frac{\gamma_1 - \gamma_2}{2} \frac{\text{Im} \mu_2}{\text{Re} \mu_2}, \quad \mathcal{E}_2 = \mathcal{E}_{EP} \equiv \pm \frac{\gamma_1 - \gamma_2}{2 \text{Re} \mu_2}, \quad (11)$$

where $\Delta \equiv E_2 - E_1 - \hbar\omega_2$ denotes the pump-frequency offset from the energy splitting between the two AI states (see SI for details). When the pump amplitude exceeds the critical value of \mathcal{E}_{EP} , the ionization peak splits into two since the dressed-state energies, $\text{Re}[\epsilon_{\pm}]$, become non degenerate. Similar to our conclusion here, Ref. 19 also states that the splitting of the lines occurs when “the dipole coupling is strong enough to compete with the autoionizing width.” However, our non-Hermitian approach enables to identify this point as an EP and, therefore, opens the possibility of exploring EP-related effects.

To summarize, we presented an *ab-initio* theory of resonant photoionization. Our theory produces accurate formulas for the ionization spectrum, which are of current interest due to recent developments in experimental capabilities for probing and controlling ionization processes. By using NHQM, our theory avoids the need of computing the continuum states, which are required by the traditional Feshbach formalism. As an application of our theory, we derive a simple expression for the Fano asymmetry factor. Moreover, we study autoionization in laser driven systems and show that the splitting of spectral lines occurs at EPs. This work opens several directions for future study. One example is finding practical applications for EPs in controlling autoionization. The non-trivial topological phase associated with the EP⁴⁰ can be used to transition between nearly degenerate states in a topologically protected manner⁴¹. Our preliminary calculations show that this effect can be used to obtain topological control of the autoionization rate. Another example for an EP-related effect is the enhanced density of states at the EP. Previous work on spontaneous emission^{28,42} shows that the emission rate can be significantly enhanced by placing the emitter near pumped resonators with EPs (i.e., using systems that have optical gain). Along similar lines, one can expect enhanced autoionization rates in systems with gain of atomic population in particular AI states. Such a situation can be engineered, for example, by considering a more complicated set of atomic transitions and lasers with recycling transitions⁴³. Finally, the present work treated broadening of absorption lines due to autoionization, but can be extended to include other line-broadening mechanism (such as vibrational and Doppler broadening) by combining NHQM with a Lindbladian formulation.

ACKNOWLEDGMENTS

AP is partially supported by an Aly Kaufman Fellowship at the Technion. NM acknowledges the financial support of I-Core: The Israeli Excellence Center “Circle of Light,” and of the Israel Science Foundation Grant No. 1530/15. PRK acknowledges the financial support by the Czech Ministry of Ed-

ucation, Youth and Sports, program INTER-EXCELLENCE (Grant LTT17015). Finally, the authors thank Christiana Koch, Michael Rosenbluh, Hossein Sadeghpour, Uri Peskin, Saar Rahav, Gad Bahir, and Ofer Neufeld for insightful discussions.

APPENDICES

Appendix A: Green's function Near EPs

Near an EP, the non-Hermitian normal-mode expansion formula for the Green's function [Eq. (4)] breaks down. In this appendix, we review the derivation of the modified expansion formula which is valid at the EP, following²⁸. Consider the parameter-dependent Hamiltonian:

$$H(\xi) = H_0 + \xi V \quad (\text{A1})$$

where H_0 is defective (i.e., the point $\xi = 0$ is an EP in parameter space). At the EP, the set of eigenvectors is no longer a complete basis of the Hilbert space. To remedy this problem, we introduce additional Jordan vectors. At a second-order EP, the Jordan vector $|j_{\text{EP}}\rangle$ is defined via the chain relations

$$\begin{aligned} H_0|\phi_{\text{EP}}\rangle &= \varepsilon_{\text{EP}}|\phi_{\text{EP}}\rangle, \\ H_0|j_{\text{EP}}\rangle &= \varepsilon_{\text{EP}}|j_{\text{EP}}\rangle + |\phi_{\text{EP}}\rangle. \end{aligned} \quad (\text{A2})$$

where ε_{EP} and ϕ_{EP} are the degenerate eigenvalue and eigenvector and the self-orthogonality condition $[(\phi_{\text{EP}}|\phi_{\text{EP}}) = 0]$ is automatically satisfied. Following⁴⁴, we choose the normalization conditions $(\phi_{\text{EP}}|j_{\text{EP}}) = \varepsilon_{\text{EP}}^{-1}$ and $(j_{\text{EP}}|j_{\text{EP}}) = 0$. Near the EP at $\xi = 0$, the Hamiltonian $H(\xi)$ has a pair of nearly degenerate eigenenergies and nearly parallel eigenvectors. They can be approximated by a Puiseux series, which contains fractional powers in the small parameter ξ ⁴⁴:

$$\begin{aligned} \varepsilon_{\pm} &= \varepsilon_{\text{EP}} + \sqrt{\xi} \mathcal{V} + \mathcal{O}(\xi) \\ |\phi_{\pm}\rangle &= |\phi_{\text{EP}}\rangle + \sqrt{\xi} \mathcal{V} |j_{\text{EP}}\rangle + \mathcal{O}(\xi) \end{aligned} \quad (\text{A3})$$

where

$$\mathcal{V} = \sqrt{\frac{(j_{\text{EP}}|V|\phi_{\text{EP}})}{(j_{\text{EP}}|\phi_{\text{EP}})}}. \quad (\text{A4})$$

Now, let us return to the modal expansion formula of G [Eq. (4)], which is valid for $\xi \neq 0$. Near the EP, the expansion is dominated by the two terms of the coalescing resonances. Keeping just these two terms in the sum, we can write

$$G(\varepsilon) = \frac{1}{\varepsilon - \varepsilon_+} \frac{|\phi_+\rangle(\phi_+|)}{(\phi_+|\phi_+)} + \frac{1}{\varepsilon - \varepsilon_-} \frac{|\phi_-\rangle(\phi_-|)}{(\phi_-|\phi_-)} \quad (\text{A5})$$

Next, we substitute the approximate expressions for $|\phi_{\pm}\rangle$ and ε_{\pm} [Eq. (A3)] into Eq. (A5) and, by carefully taking the limit of $\xi \rightarrow 0$, we obtain²⁸

$$\begin{aligned} G(\varepsilon) &= \frac{1}{(\varepsilon - \varepsilon_{\text{EP}})^2} \frac{|\phi_{\text{EP}}\rangle(\phi_{\text{EP}}|}{(\phi_{\text{EP}}|j_{\text{EP}})} + \\ &\frac{1}{\varepsilon - \varepsilon_{\text{EP}}} \left(\frac{|\phi_{\text{EP}}\rangle(j_{\text{EP}}|}{(\phi_{\text{EP}}|j_{\text{EP}})} + \frac{|j_{\text{EP}}\rangle(\phi_{\text{EP}}|}{(\phi_{\text{EP}}|j_{\text{EP}})} \right) \end{aligned} \quad (\text{A6})$$

The double pole at ε_{EP} dominates the absorption spectrum near the EP.

Appendix B: Non-Hermitian Fano factor

In this appendix, we derive Eq. (7) from the main text. The formula is obtained by comparing the ratio of the symmetric and antisymmetric parts of our new spectral formula [Eq. (5)] and the Fano lineshape near a single resonance [Eq. (6)]. First, let us introduce the dimensionless detuning parameter $x = \frac{\omega - \Omega}{\gamma/2}$ and rewrite Eq. (6) as

$$S_F = 1 + \frac{2xq}{x^2 + 1} + \frac{q^2 - 1}{x^2 + 1} \quad (\text{B1})$$

Next, let us define the symmetric and antisymmetric parts of our absorption formula as

$$\begin{aligned} S_{\text{symm}} &= \frac{|\mathcal{E}|^2}{\hbar\pi} \frac{\text{Re} \mu_{if}^2 \text{Im} \varepsilon_f}{(\omega - \text{Re} \varepsilon_f)^2 + (\text{Im} \varepsilon_f)^2}, \\ S_{\text{asymm}} &= \frac{|\mathcal{E}|^2}{\hbar\pi} \frac{\text{Im} \mu_{if}^2 (\text{Re} \varepsilon_f - \omega)}{(\omega - \text{Re} \varepsilon_f)^2 + (\text{Im} \varepsilon_f)^2}, \end{aligned} \quad (\text{B2})$$

where introduced the shorthand notation $\mu_{if}^2 = (\phi_i^L|x|\phi_f^R)(\phi_f^L|x|\phi_i^R)$. By comparing Eq. (B1) and Eq. (B2) we find that

$$\frac{2q}{q^2 - 1} = \frac{\text{Im} \mu_{if}^2}{\text{Re} \mu_{if}^2}. \quad (\text{B3})$$

The solution of Eq. (B3) yields the Fano asymmetry factor [Eq. (7)]. The sign of q is determined by the sign of $\text{Im} \mu_{if}^2$. When $q > 0$, the absorption is stronger at frequencies higher than the resonance frequency and weaker below the resonance. When $q < 0$, the contrary is true.

Appendix C: Absorption in laser-driven systems

1. The Floquet Hamiltonian

In this section, we explain how to construct the Floquet Hamiltonian and find its eigenvalues and eigenvectors, which appear in Eq. (9) in the main text. We wish to solve the Floquet eigenvalue problem

$$\mathcal{H} \Phi_\alpha = \varepsilon_\alpha \Phi_\alpha, \quad (\text{C1})$$

where

$$\mathcal{H} \equiv H_0 + \mathcal{E} x \cos \omega_0 t - i \hbar \partial_t. \quad (\text{C2})$$

In order to solve Eq. (C1) numerically, we introduce M temporal Fourier basis states, $f_m(t) = e^{i\omega_m t}$, and N spatial field-free states, $\phi_\mu^{\text{FF}}(x)$. Invoking the completeness relation,

$$1 = \sum_{m=1}^M |f_m(t)\rangle \langle f_m(t)| \otimes \sum_{\mu=1}^N |\phi_\mu^{\text{R,FF}}(x)\rangle \langle \phi_\mu^{\text{L,FF}}(x)|, \quad (\text{C3})$$

we can rewrite Eq. (C1) in matrix form:

$$\sum_{m,\nu} (n, \nu | \mathcal{H} | m, \mu) (m, \mu | \Phi_\alpha) = \varepsilon_\alpha (n, \nu | \Phi_\alpha) \quad (\text{C4})$$

or in shorthand notation:

$$\overline{\overline{\mathcal{H}}} \vec{\Phi}_\alpha = \varepsilon_\alpha \vec{\Phi}_\alpha, \quad (\text{C5})$$

where $\overline{\overline{\mathcal{H}}}$ is block diagonal, with block size $M \times M$. The diagonal blocks are associated with the first and last terms in Eq. (C2)

$$\overline{\overline{\mathcal{H}}} \mu n, \nu n = (\varepsilon_\mu^{\text{FF}} + n\hbar\omega_0) \delta_{\mu,\nu} \quad (\text{C6})$$

and the off-diagonal elements come from the second term:

$$\overline{\overline{\mathcal{H}}} \mu n, \nu n \pm 1 = \frac{\mathcal{E}}{2} (\phi_\mu^{\text{L,FF}} | x | \phi_\nu^{\text{R,FF}}) \quad (\text{C7})$$

2. Fermi-Floquet absorption formula

In this appendix, we derive Eq. (9) from the main text. Our derivation is inspired by Ref.³⁶, which analyzes scattering from a time-periodic potential. Consider an atom or molecule, which interacts with a laser at frequency ω_0 . The system is described by the Hamiltonian H_0 , whose eigenstates are Floquet states, as explained in the main text. The propagator of H_0 is defined via

$$i\hbar \partial_t U_0(t_0, t) = H_0(t) U_0(t_0, t). \quad (\text{C8})$$

We also introduce a weak laser, hereafter called “the probe,” with frequency ω . The total Hamiltonian is

$$H = H_0 + V, \quad (\text{C9})$$

where the interaction term is $V = \mathcal{E} x e^{i\omega t}$. In order to derive Fermi-Floquet golden rule, we move to the interaction picture, where states and operators are defined as

$$\begin{aligned} |\Psi^I(t)\rangle &= U_0(t, t_0) |\Psi(t)\rangle \\ \mathcal{O}^I(t) &= U_0(t, t_0) \mathcal{O} U_0(t_0, t). \end{aligned} \quad (\text{C10})$$

Note that the total propagator, defined as

$$i\hbar \partial_t U(t_0, t) = H(t) U(t_0, t), \quad (\text{C11})$$

can be written as a product of the unperturbed and interaction-picture propagators:

$$U(t_0, t) = U_0(t_0, t) U^I(t_0, t). \quad (\text{C12})$$

The last statement can be verified by substituting Eq. (C12) into Eq. (C11), applying the chain rule to compute $\partial_t U(t, t_0)$, and using Eq. (C8) and $V^I = U_0(t, t_0) V U_0(t_0, t)$.

Next, we compute the transition amplitude between Floquet states $|\Psi_f(t)\rangle$ and $|\Psi_i(t)\rangle$, where i and f are super-indexes

which denote the field-free state and the channel. The transition amplitude is

$$\begin{aligned} A(i \rightarrow f, t) &= (\Psi_f(t) | U(0, t) | \Psi_i(0)) = \\ &= (\Psi_f(t) | U_0(0, t) U^I(0, t) | \Psi_i(0)) = \\ &= (\Psi_f(0) | U^I(0, t) | \Psi_i(0)) \end{aligned} \quad (\text{C13})$$

We use a Dyson series to express the interaction-picture propagator, U^I , in terms of V^I . Keeping terms up to the first order in V^I , one obtains:

$$U^I(t_0, t) = \mathbb{1} - \frac{i}{\hbar} \int_{t_0}^t dt' V^I(t') + \mathcal{O}(V^2). \quad (\text{C14})$$

Substituting Eq. (C14) into Eq. (C13), one obtains

$$\begin{aligned} A(i \rightarrow f, t) &= \frac{-i}{\hbar} \int_0^t dt' (\Psi_f(0) | V^I(0, t') | \Psi_i(0)) = \\ &= \frac{-i}{\hbar} \int_0^t dt' (\Psi_f(0) | U_0(t', 0) V U_0(0, t') | \Psi_i(0)) = \\ &= \frac{-i}{\hbar} \int_0^t dt' e^{-i(\varepsilon_i - \varepsilon_f)t'/\hbar} (\Phi_f(t') | V | \Phi_i(t')). \end{aligned} \quad (\text{C15})$$

Since the Floquet states $\Phi_\alpha(x, t)$ are periodic in time, one can decompose them into Fourier components

$$\Phi_\alpha(x, t) = \sum_n e^{i\omega_0 n t} \tilde{\Phi}_{\alpha,n}(x) \quad (\text{C16})$$

where the Fourier components of the wavefunction are $\tilde{\Phi}_{\alpha,n}(x) \equiv \frac{1}{\sqrt{2\pi}} \int_{-\infty}^{\infty} dt \Phi_\alpha(x, t) e^{-i\omega_0 n t}$. Using this expansion, the transition amplitude becomes

$$\begin{aligned} A(i \rightarrow f, t) &= \\ &= \sum_{mn} \frac{-i\mathcal{E}}{\hbar} \int_0^t dt' e^{-i(\varepsilon_i - \varepsilon_f - (n-m)\hbar\omega_0 - \hbar\omega)t'/\hbar} (\tilde{\Phi}_{f,n} | x | \tilde{\Phi}_{i,m}) = \\ &= \mathcal{E} \sum_{mn} \frac{e^{-i(\varepsilon_i - \varepsilon_f - m\hbar\omega_0 - \hbar\omega)t/\hbar} - 1}{\varepsilon_i - \varepsilon_f - m\hbar\omega_0 - \hbar\omega} (\tilde{\Phi}_{f,m+n} | x | \tilde{\Phi}_{i,m}). \end{aligned} \quad (\text{C17})$$

The absorption spectrum can be found by taking the time average of the transition probability:

$$S(\omega) \equiv \frac{1}{T} \int_0^T dt \frac{d}{dt} |A_{if}|^2 = 2\text{Re} \left[\frac{1}{T} \int_0^T dt A^* \frac{dA}{dt} \right], \quad (\text{C18})$$

where T is a large integer multiple of the oscillation period $\frac{2\pi}{\omega_0}$. Substituting Eq. (C17) into Eq. (C18) and neglecting rapidly oscillating terms, we obtain

$$\frac{1}{T} \int_0^T dt A^* \frac{dA}{dt} = \frac{-i|\mathcal{E}|^2}{\hbar} \sum_{m\ell} \frac{(\tilde{\Phi}_{f,m+n} | x | \tilde{\Phi}_{i,m})(\tilde{\Phi}_{i,m} | x | \tilde{\Phi}_{f,m+\ell})}{(\varepsilon_i - \varepsilon_f - m\hbar\omega_0 - \hbar\omega)} \quad (\text{C19})$$

Finally, we take the real part of Eq. (C19) and arrive at

$$S(\omega) = \frac{|\mathcal{E}|^2}{\hbar} \text{Im} \left[\sum_{m\ell} \frac{(\tilde{\Phi}_{f,m+n}^L | x | \tilde{\Phi}_{i,m}^R)(\tilde{\Phi}_{i,\ell}^L | x | \tilde{\Phi}_{f,\ell+m}^R)}{\varepsilon_i - \varepsilon_f - m\hbar\omega_0 - \hbar\omega} \right] \quad (\text{C20})$$

The last formula can be rewritten compactly as Eq. (9) in the main text.

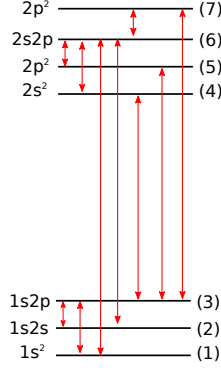


TABLE S1. Complex energies

| | | Re[E] ⁴⁵ | Re[E] ¹⁶ | Im[E] ⁴⁵ | Im[E] ¹⁶ |
|---|-----------------|---------------------|---------------------|---------------------|---------------------|
| 1 | 1s ² | -2.90372 | -2.9035 | 0 | 0 |
| 2 | 1s2s | -2.14597 | -2.1460 | 0 | 0 |
| 3 | 1s2p | -2.12384 | -2.1238 | 0 | 0 |
| 4 | 2s ² | -0.777868 | -0.7779 | 0.002271 | -0.0023 |
| 5 | 2p ² | -0.710500 | -0.7018 | 0.001181 | -0.0012 |
| 6 | 2s2p | -0.693135 | -0.6930 | 0.0006865 | -0.0007 |
| 7 | 2p ² | -0.621926 | -0.6216 | 0.000108 | -0.0001 |

TABLE S2. Transition dipole moments

| | μ_R^{16} | μ_I^{16} | λ [nm] |
|-----------------------|--------------|--------------|------------------|
| 1 \leftrightarrow 3 | 0.4207 | 0.00000189 | 58.44 (UV) |
| 1 \leftrightarrow 6 | 0.03599 | 0.01299 | 20.61 (UV) |
| 2 \leftrightarrow 3 | 2.9167 | 0.000004652 | 2058.47 (IR) |
| 2 \leftrightarrow 6 | 0.3130 | -0.003598 | 31.36 (UV) |
| 3 \leftrightarrow 4 | -0.1231 | -0.002554 | 33.85 (UV) |
| 3 \leftrightarrow 5 | 0.3288 | 0.000193 | 32.04 (UV) |
| 3 \leftrightarrow 7 | -0.1925 | 0.0003475 | 30.33 (UV) |
| 4 \leftrightarrow 6 | 1.5227 | -0.00973 | 536.95 (visible) |
| 5 \leftrightarrow 6 | 1.70545 | -0.003767 | 5160.2 (IR) |
| 6 \leftrightarrow 7 | -2.1614 | -0.001007 | 638.15 (visible) |

Fig. S1: Schematic drawing of the Hartree-Fock orbitals of helium (left). Table S1: The *ab-initio* complex eigenenergies used in Fig. 3 in the main text. For comparison, we also show the results of ⁴⁵. Table S2: Complex transition dipole moments¹⁶.

3. Autoionization spectral formula in the field-free basis

In order to evaluate our new formula for the absorption spectrum [Eq. (C20) or equivalently Eq. (9) in the main text], we need to know the Fourier transforms of Floquet states. However, standard quantum chemistry methods solve the field-free problem, and we would like to use the field-free basis states and avoid the formidable task of solving the Floquet eigenvalue problem for a multielectron atom or molecule. To this end, we expand the Fourier transforms of the Floquet states in the basis of field-free states.

$$|\tilde{\phi}_{\alpha,n}\rangle = \sum_{\mu} (\phi_{\mu}^{\text{FF}} | \tilde{\phi}_{\alpha,n} \rangle | \phi_{\mu}^{\text{FF}} \rangle \quad (\text{C21})$$

Substituting Eq. (C21) into Eq. (C20), we obtain

$$S(\omega) = \frac{|\mathcal{E}|^2}{\hbar} \text{Im} \left[\sum_{\substack{mn\ell \\ \mu\nu\sigma\tau}} (\tilde{\phi}_{i,\ell}^L | \phi_{\tau}^{\text{FF}} \rangle) (\phi_{\tau}^{\text{FF}} | x | \phi_{\sigma}^{\text{FF}} \rangle) \frac{(\phi_{\sigma}^{\text{FF}} | \tilde{\phi}_{f,\ell+m}^R \rangle) (\tilde{\phi}_{f,n+m}^L | \phi_{\mu}^{\text{FF}} \rangle)}{\varepsilon_i - \varepsilon_f - m\hbar\omega_0 - \hbar\omega} (\phi_{\mu}^{\text{FF}} | x | \phi_{\nu}^{\text{FF}} \rangle) (\phi_{\nu}^{\text{FF}} | \tilde{\phi}_{i,n}^R \rangle) \right] \quad (\text{C22})$$

The transition dipole moments between field-free states, $(\phi_{\tau}^{\text{FF}} | x | \phi_{\sigma}^{\text{FF}} \rangle)$, are obtained directly from available quantum chemistry codes. By construction, the expansion coefficients, $(\phi_{\mu}^{\text{FF}} | \tilde{\phi}_{\alpha,n}^R \rangle)$, are the components of the eigenvectors of the Floquet matrix:

$$(\phi_{\mu}^{\text{L,FF}} | \tilde{\phi}_{\alpha,m}^R \rangle) = (m, \mu | \Phi_{\alpha}^R \rangle). \quad (\text{C23})$$

The eigenvectors of the Floquet Hamiltonian, $(m, \mu | \Phi_{\alpha}^R \rangle)$, are defined in Eq. (C4).

4. EPs in the Floquet Hamiltonian

To get an initial guess for the location of the EP, it is convenient to project the full Hamiltonian onto the field-free excited states ψ_2 and ψ_3 and use the rotating wave approximation, which gives the 2×2 Hamiltonian

$$H_{\text{exc}} = \begin{pmatrix} E_2 & -\frac{\mu_{23}\mathcal{E}}{2} \\ -\frac{\mu_{32}\mathcal{E}}{2} & E_3 - \hbar\omega_0 \end{pmatrix}. \quad (\text{C24})$$

Subtracting E_2 from the diagonal and introducing the definitions $\delta \equiv \text{Re}[E_3 - E_2 - \hbar\omega_0]$ and $\Gamma \equiv -2\text{Im}[E_3 - E_2]$, we obtain

$$H_{\text{exc}} = \begin{pmatrix} 0 & -\frac{\mu_{23}\mathcal{E}}{2} \\ -\frac{\mu_{23}\mathcal{E}}{2} & \delta - i\frac{\Gamma}{2} \end{pmatrix}. \quad (\text{C25})$$

The characteristic polynomial of H_{exc} is

$$f(x) = x^2 - x(\delta - i\frac{\Gamma}{2}) - \frac{(\mu_{23}\mathcal{E})^2}{4}, \quad (\text{C26})$$

and EPs occur when the discriminant of the polynomial vanishes:

$$\Delta^2 \equiv (\frac{\delta}{2} - i\frac{\Gamma}{4})^2 + \frac{(\mu_{23}\mathcal{E})^2}{4} = 0 \quad (\text{C27})$$

Solving for \mathcal{E} and δ , we obtain the critical values³⁹:

$$\delta_{\text{EP}} = \frac{\Gamma \text{Im} \mu_{23}}{2 \text{Re} \mu_{23}} \quad \mathcal{E}_{\text{EP}} = \pm \frac{\Gamma}{2 \text{Re} \mu_{23}} \quad (\text{C28})$$

In the numerical calculation, we found EPs in the large $(MN \times MN)$ Floquet Hamiltonian, including four field-free

basis states and five Floquet bands, but found that the EP is obtained near the EP of the approximate 2×2 model. Specifically, we find an EP of the full Floquet Hamiltonian at $\delta \approx 1.001645 \delta_{\text{EP}}$ and $\mathcal{E} \approx 0.99420 \mathcal{E}_{\text{EP}}$.

Appendix D: Electronic-structure of He

Figures S1 presents the energy levels, lifetimes, and transition dipole moments between the lowest-energy single- and double-excitation states in helium. The numerical values, summarized in Table S1–S2, were obtained by Kaprálová-Žďánská *et. al.*¹⁶, and are used in all the calculations in the main text.

- ¹F. Krausz and M. Ivanov, “Attosecond physics,” *Rev. Mod. Phys.* **81**, 163 (2009).
- ²J. Itatani, J. Levesque, D. Zeidler, H. Niikura, H. Pépin, J. C. Kieffer, P. B. Corkum, and D. M. Villeneuve, “Tomographic imaging of molecular orbitals,” *Nature* **432**, 867 (2004).
- ³P. M. Paul, E. S. Toma, P. Breger, G. Mullot, F. Augé, P. Balcou, H. G. Muller, and P. Agostini, “Observation of a train of attosecond pulses from high harmonic generation,” *Science* **292**, 1689–1692 (2001).
- ⁴K. Klünder, J. M. Dahlström, M. Gisselbrecht, T. Fordell, M. Swoboda, D. Guenot, P. Johnsson, J. Caillat, J. Mauritsson, A. Maquet, J. Caillat, J. Mauritsson, A. Maquet, , and R. Taieb, “Probing single-photon ionization on the attosecond time scale,” *Phys. Rev. Lett.* **106**, 143002 (2011).
- ⁵D. Azoury, M. Krüger, G. Orenstein, H. R. Larsson, S. Bauch, B. D. Bruner, and N. Dudovich, “Self-probing spectroscopy of xuv photoionization dynamics in atoms subjected to a strong-field environment,” *Nature Comm.* **8**, 1453 (2017).
- ⁶H. Feshbach, “A unified theory of nuclear reactions. ii,” *Ann. Phys.* **19**, 287–313 (1962).
- ⁷H. Friedrich and D. Wintgen, “Interfering resonances and bound states in the continuum,” *Phys. Rev. A* **32**, 3231 (1985).
- ⁸V. Averbukh and L. S. Cederbaum, “Ab-initio calculation of interatomic decay rates by a combination of the fano ansatz, green’s-function methods, and the stieljes imaging technique,” *J. Chem. Phys.* **123**, 204107 (2005).
- ⁹R. E. Goetz, T. A. Isaev, B. Nikoobakht, R. Berger, and C. P. Koch, “Theoretical description of circular dichroism in photoelectron angular distributions of randomly oriented chiral molecules after multi-photon photoionization,” *J. Chem. Phys.* **146**, 024306 (2017).
- ¹⁰N. Moiseyev, *Non-Hermitian Quantum Mechanics* (Cambridge University Press, 2011).
- ¹¹U. Fano, “Effects of configuration interaction on intensities and phase shifts,” *Phys. Rev.* **124**, 1866 (1961).
- ¹²S. H. Autler and C. H. Townes, “Stark effect in rapidly varying fields,” *Phys. Rev.* **100**, 703 (1955).
- ¹³T. Kato, *Perturbation theory for linear operators*, Vol. 132 (Springer Science & Business Media, 2013).
- ¹⁴D. Zuev, T.-C. Jagau, K. B. Bravaya, E. Epifanovsky, Y. Shao, E. Sundstrom, M. Head-Gordon, and A. I. Krylov, “Complex absorbing potentials within eom-cc family of methods: Theory, implementation, and benchmarks,” *J. Chem. Phys.* **141**, 024102 (2014).
- ¹⁵A. Landau, I. Haritan, P. R. Kapralova-Zdanska, and N. Moiseyev, “Atomic and molecular complex resonances from real eigenvalues using standard (hermitian) electronic structure calculations,” *J. Phys. Chem. A* **120**, 3098–3108 (2016).
- ¹⁶P. R. Kaprálová-Žďánská, J. Šmydke, and S. Civiš, “Excitation of helium rydberg states and doubly excited resonances in strong extreme ultraviolet fields: Full-dimensional quantum dynamics using exponentially tempered gaussian basis sets,” *J. Chem. Phys.* **139**, 104314 (2013).
- ¹⁷P. R. Kaprálová-Žďánská and J. Šmydke, “Gaussian basis sets for highly excited and resonance states of helium,” *J. Chem. Phys.* **138**, 024105 (2013).
- ¹⁸T. Fukuta, S. Garmon, K. Kanki, K.-I. Noba, and S. Tanaka, “Fano absorption spectrum with the complex spectral analysis,” *Phys. Rev. A* **96**, 052511 (2017).
- ¹⁹N. E. Karapanagioti, O. Faucher, Y. L. Shao, D. Charalambidis, H. Bachau, and E. Cormier, “Observation of autoionization suppression through coherent population trapping,” *Phys. Rev. Lett.* **74**, 2431 (1995).
- ²⁰N. E. Karapanagioti, D. Charalambidis, C. J. G. J. Uiterwaal, C. Fotakis, H. Bachau, I. Sánchez, and E. Cormier, “Effects of coherent coupling of autoionizing states on multiphoton ionization,” *Phys. Rev. A* **53**, 2587 (1996).
- ²¹T. Halfmann, L. P. Yatsenko, M. Shapiro, B. W. Shore, and K. Bergmann, “Population trapping and laser-induced continuum structure in helium: Experiment and theory,” *Phys. Rev. A* **58**, R46 (1998).
- ²²J. Y. Gao, S. H. Yang, D. Wang, X. Z. Guo, K. X. Chen, Y. Jiang, and B. Zhao, “Electromagnetically induced inhibition of two-photon absorption in sodium vapor,” *Phys. Rev. A* **61**, 023401 (2000).
- ²³H. Bachau, P. Lambropoulos, and R. Shakeshaft, “Theory of laser-induced transitions between autoionizing states of he,” *Phys. Rev. A* **34**, 4785 (1986).
- ²⁴Y. J. Yan and S. Mukamel, “Eigenstate-free, green function, calculation of molecular absorption and fluorescence line shapes,” *J. Chem. Phys.* **85**, 5908–5923 (1986).
- ²⁵S. Mukamel, *Principles of Nonlinear Optical Spectroscopy* (Oxford University Press on Demand, 1999).
- ²⁶A. Shibata and Y. Toyozawa, “Antiresonance in the optical absorption spectra of the impurity in solids,” *J. Phys. Soc. Jpn.* **25**, 335–345 (1968).
- ²⁷G. B. Arfken and H. J. Weber, *Mathematical Methods for Physicists* (Elsevier Academic Press, 2006) pp. 184–185.
- ²⁸A. Pick, B. Zhen, O. D. Miller, C. W. Hsu, F. Hernandez, A. W. Rodriguez, M. Soljacic, and S. G. Johnson, “General theory of spontaneous emission near exceptional points,” *Opt. Exp.* **25**, 12325–12348 (2017).
- ²⁹D. J. Griffiths, *Introduction to quantum mechanics* (Upper Saddle River, NJ: Pearson Prentice Hall, 2005).
- ³⁰K. M. Lee, P. T. Leung, and K. M. Pang, “Dyadic formulation of morphology-dependent resonances. i. completeness relation,” *JOSA B* **16**, 1409–1417 (1999).
- ³¹P. T. Leung, S. Y. Liu, and K. Young, “Completeness and orthogonality of quasinormal modes in leaky optical cavities,” *Phys. Rev. A* **49**, 3057 (1994).
- ³²G. W. Hanson, A. I. Nosich, and E. M. Kartchevski, “Green’s function expansions in dyadic root functions for shielded layered waveguides,” *PIER* **39**, 61–91 (2003).
- ³³E. Hernandez, A. Jauregui, and A. Mondragon, “Degeneracy of resonances in a double barrier potential,” *J. Phys. A* **33**, 4507–4523 (2000).
- ³⁴E. Hernández, A. Jauregui, and A. Mondragon, “Jordan blocks and Gamow-Jordan eigenfunctions associated with a degeneracy of unbound states,” *Phys. Rev. A* **67**, 022721 (2003).
- ³⁵T. Dittrich, P. Hänggi, G.-L. Ingold, B. Kramer, G. Schön, and W. Zwerger, “Quantum transport and dissipation,” (Wiley-Vch Weinheim, 1998) Chap. 5.
- ³⁶T. Bilitewski and N. R. Cooper, “Scattering theory for floquet-bloch states,” *Phys. Rev. A* **91**, 033601 (2015).
- ³⁷S. I. Chu and W. P. Reinhardt, “Intense field multiphoton ionization via complex dressed states: Application to the h atom,” *Phys. Rev. Lett.* **39**, 1195 (1977).
- ³⁸S. I. Chu, “Recent developments in semiclassical floquet theories for intense-field multiphoton processes,” in *Adv. At. Mol. Phys.*, Vol. 21 (Elsevier, 1985) pp. 197–253.
- ³⁹P. R. Kaprálová-Žďánská and N. Moiseyev, “Helium in chirped laser fields as a time-asymmetric atomic switch,” *J. Chem. Phys.* **141**, 014307 (2014).
- ⁴⁰A. A. Mailybaev, O. N. Kirillov, and A. P. Seyranian, “Geometric phase around exceptional points,” *Phys. Rev. A* **72**, 014104 (2005).
- ⁴¹J. Doppler, A. A. Mailybaev, J. Bohm, U. Kuhl, A. Girschik, F. Libisch, T. J. Milburn, P. Rabl, N. Moiseyev, and S. Rotter, “Dynamically encircling an exceptional point for asymmetric mode switching,” *Nature* **537**, 76–79 (2016).
- ⁴²Z. Lin, A. Pick, M. Lončar, and A. W. Rodriguez, “Enhanced spontaneous emission at third-order dirac exceptional points in inverse-designed photonic crystals,” *Phys. Rev. Lett.* **117**, 107402 (2016).
- ⁴³E. Togan, Y. Chu, A. Imamoglu, and M. D. Lukin, “Laser cooling and real-time measurement of the nuclear spin environment of a solid-state qubit,” *Nature* **478**, 497 (2011).

- ⁴⁴A. P. Seyranian and A. A. Mailybaev, *Multiparameter Stability Theory With Mechanical Applications* (World Scientific Publishing, 2003).
- ⁴⁵I. Gilary, P. R. Kaprálová-Žďánská, and N. Moiseyev, “*Ab-initio* calculation of harmonic generation spectra of helium using a time-dependent non-hermitian formalism,” *Phys. Rev. A* **74**, 052505 (2006).
- ⁴⁶P. Lambropoulos and P. Zoller, “Autoionizing states in strong laser fields,” *Phys. Rev. A* **24**, 379 (1981).
- ⁴⁷B. D. Bruner, M. Krüger, O. Pedatzur, G. Orenstein, D. Azoury, and N. Dudovich, “Robust enhancement of high harmonic generation via attosecond control of ionization,” *Opt. Express* **26**, 9310–9322 (2018).
- ⁴⁸S. Beaulieu, A. Comby, A. Clergerie, J. Caillat, D. Descamps, N. Dudovich, B. Fabre, R. Géraud, F. Légaré, S. Petit, and B. Pons, “Attosecond-resolved photoionization of chiral molecules,” *Science* **358**, 1288–1294 (2017).
- ⁴⁹X. Zhang, N. Xu, K. Qu, Z. Tian, R. Singh, J. Han, G. S. Agarwal, and W. Zhang, “Electromagnetically induced absorption in a three-resonator metasurface system,” *Sci. Rep.* **5**, 10737 (2015).
- ⁵⁰J. Gu, R. Singh, X. Liu, X. Zhang, Y. Ma, S. Zhang, S. A. Maier, Z. Tian, A. K. Azad, H.-T. Chen, A. J. Taylor, J. Han, and W. Zhang, “Active control of electromagnetically induced transparency analogue in terahertz metamaterials,” *Nat. Comm.* **3**, 1151 (2012).
- ⁵¹S. E. Harris, “Electromagnetically induced transparency,” *Phys. Today* **50**, 36 (1997).
- ⁵²A. Kuzmich, W. P. Bowen, A. D. Boozer, A. Boca, C. W. Chou, L.-M. Duan, and H. J. Kimble, “Generation of nonclassical photon pairs for scalable quantum communication with atomic ensembles,” *Nature* **423**, 731 (2003).
- ⁵³P. R. Hemmer, D. P. Katz, J. Donoghue, M. Cronin-Golomb, M. S. Shahriar, and P. Kumar, “Efficient low-intensity optical phase conjugation based on coherent population trapping in sodium,” *Opt. Lett.* **20**, 982–984 (1995).
- ⁵⁴M. D. Lukin and A. Imamoglu, “Controlling photons using electromagnetically induced transparency,” *Nature* **413**, 273 (2001).
- ⁵⁵G. Alzetta, A. Gozzini, L. Moi, and G. Orriols, “An experimental method for the observation of rf transitions and laser beat resonances in oriented vapour,” *Il Nuovo Cimento B* **36**, 5–20 (1976).
- ⁵⁶K. H. Hahn, D. A. King, and S. E. Harris, “Nonlinear generation of 104.8-nm radiation within an absorption window in zinc,” *Phys. Rev. Lett.* **65**, 2777 (1990).
- ⁵⁷M. Fleischhauer, A. Imamoglu, and J. P. Marangos, “Electromagnetically induced transparency: Optics in coherent media,” *Rev. Mod. Phys.* **77**, 633 (2005).
- ⁵⁸S. Gilbertson, M. Chini, X. Feng, S. Khan, Y. Wu, and Z. Chang, “Monitoring and controlling the electron dynamics in helium with isolated attosecond pulses,” *Phys. Rev. Lett.* **105**, 263003 (2010).
- ⁵⁹W.-C. Chu, S.-F. Zhao, and C. D. Lin, “Laser-assisted-autoionization dynamics of helium resonances with single attosecond pulses,” *Phys. Rev. A* **84**, 033426 (2011).
- ⁶⁰L. V. Hau, S. E. Harris, Z. Dutton, and C. H. Behroozi, “Light speed reduction to 17 metres per second in an ultracold atomic gas,” *Nature* **397**, 594 (1999).
- ⁶¹C. Goren, A. D. Wilson-Gordon, M. Rosenbluh, and H. Friedmann, “Electromagnetically induced absorption due to transfer of coherence and to transfer of population,” *Phys. Rev. A* **67**, 033807 (2003).
- ⁶²A. Lezama, S. Barreiro, and A. M. Akulshin, “Electromagnetically induced absorption,” *Phys. Rev. A* **59**, 4732 (1999).
- ⁶³M. O. Scully and M. S. Zubairy, *Quantum Optics* (Cambridge University Press, 1997).
- ⁶⁴K. J. Boller, A. Imamoglu, and S. E. Harris, “Observation of electromagnetically induced transparency,” *Physical Review Letters* **66**, 2593 (1991).
- ⁶⁵T. Goldzak, A. A. Mailybaev, and N. Moiseyev, “Light stops at exceptional points,” *Phys. Rev. Lett.* **120**, 013901 (2018).
- ⁶⁶H. Menke, M. Klett, H. Cartarius, J. Main, and G. Wunner, “State flip at exceptional points in atomic spectra,” *Phys. Rev. A* **93**, 013401 (2016).
- ⁶⁷H. Cartarius, J. Main, and G. Wunner, “Exceptional points in the spectra of atoms in external fields,” *Phys. Rev. A* **79**, 053408 (2009).
- ⁶⁸H. Cartarius, J. Main, and G. Wunner, “Exceptional points in atomic spectra,” *Phys. Rev. Lett.* **99**, 173003 (2007).
- ⁶⁹M. Domke, C. Xue, A. Puschmann, T. Mandel, E. Hudson, D. A. Shirley, G. Kaindl, C. H. Greene, H. R. Sadeghpour, and H. Petersen, “Extensive double-excitation states in atomic helium,” *Phys. Rev. Lett.* **66**, 1306 (1991).
- ⁷⁰J. C. Light and T. Carrington Jr, “Discrete-variable representations and their utilization,” *Adv. Chem. Phys.* **114**, 263–310 (2000).
- ⁷¹N. Moiseyev, “Derivations of universal exact complex absorption potentials by the generalized complex coordinate method,” *J. Phys. B* **31**, 1431 (1998).
- ⁷²Y. Sajeed and N. Moiseyev, “Reflection-free complex absorbing potential for electronic structure calculations: Feshbach-type autoionization resonances of molecules,” *J. Chem. Phys.* **127**, 034105 (2007).
- ⁷³M. D. Frogley, J. F. Dynes, M. Beck, J. Faist, and C. C. Phillips, “Gain without inversion in semiconductor nanostructures,” *Nat. Mater.* **5**, 175 (2006).
- ⁷⁴A. Temkin and A. K. Bhatia, “Theory and calculation of resonances and autoionization of two-electron atoms and ions,” in *Autoionization* (Springer, 1985) pp. 1–34.
- ⁷⁵M. V. Berry, “Mode degeneracies and the petermann excess-noise factor for unstable lasers,” *J. Mod. Opt.* **50**, 63–81 (2003).
- ⁷⁶R. G. Gordon, “Correlation functions for molecular motion,” in *Advances in Magnetic and Optical Resonance*, Vol. 3 (Elsevier, 1968) pp. 1–42.
- ⁷⁷A. D. Shiner, B. E. Schmidt, C. Trallero-Herrero, H. J. Wörner, S. Patchkovskii, P. B. Corkum, J. C. Kieffer, F. Légaré, and D. M. Villeneuve, “Probing collective multi-electron dynamics in xenon with high-harmonic spectroscopy,” *Nature Physics* **7**, 464 (2011).
- ⁷⁸V. V. Strelkov, “Attosecond-pulse production using resonantly enhanced high-order harmonics,” *Phys. Rev. A* **94**, 063420 (2016).
- ⁷⁹L. N. Trefethen and M. Embree, *Spectra and Pseudospectra: The Behavior of Nonnormal Matrices and Operators* (Princeton University Press, 2005).
- ⁸⁰C. Ott, A. Kaldun, P. Raith, K. Meyer, M. Laux, J. Evers, C. H. Keitel, C. H. Greene, and T. Pfeifer, “Lorentz meets fano in spectral line shapes: a universal phase and its laser control,” *Science* **340**, 716–720 (2013).
- ⁸¹J. Kohanoff, *Electronic structure calculations for solids and molecules: theory and computational methods* (Cambridge University Press, 2006).
- ⁸²U. Riss and H. D. Meyer, “Reflection-free complex absorbing potentials,” *J. Phys. B* **28**, 1475 (1995).
- ⁸³N. Moiseyev, “Quantum theory of resonances: calculating energies, widths and cross-sections by complex scaling,” *Phys. Rep.* **302**, 212–293 (1998).
- ⁸⁴R. Santra and L. S. Cederbaum, “Non-hermitian electronic theory and applications to clusters,” *Phys. Rep.* **368**, 1–117 (2002).
- ⁸⁵C. J. Cramer, “Essentials of computational chemistry: theories and models,” (John Wiley & Sons, 2013) Chap. 7–8.
- ⁸⁶D. J. Griffiths, “Boundary conditions at the derivative of a delta function,” *J. Phys. A Math. Gen.* **26**, 2265 (1993).
- ⁸⁷C. E. Ruter, K. G. Makris, R. El-Ganainy, D. N. Christodoulides, M. Segev, and D. Kip, “Observation of parity–time symmetry in optics,” *Nat. Phys.* **6**, 192–195 (2010).
- ⁸⁸A. Guo, G. J. Salamo, D. Duchsne, R. Morandotti, M. Volatier-Ravat, V. Aimez, G. A. Siviloglou, and D. N. Christodoulides, “Observation of \mathcal{PT} -symmetry breaking in complex optical potentials,” *Phys. Rev. Lett.* **103**, 093902 (2009).
- ⁸⁹W. D. Heiss, “The physics of exceptional points,” *J. Phys. A: Math. Theor.* **45**, 444016 (2010).
- ⁹⁰S. Klaiman, U. Gunther, and N. Moiseyev, “Visualization of branch points in \mathcal{PT} -symmetric waveguides,” *Phys. Rev. Lett.* **101**, 080402 (2008).
- ⁹¹K. G. Makris, R. El-Ganainy, D. N. Christodoulides, and Z. H. Musslimani, “Beam dynamics in \mathcal{PT} -symmetric optical lattices,” *Phys. Rev. Lett.* **100**, 103904 (2008).
- ⁹²C. M. Bender and S. Boettcher, “Real spectra in non-Hermitian hamiltonians having \mathcal{PT} -symmetry,” *Phys. Rev. Lett.* **80**, 5243 (1998).
- ⁹³M. Brandstetter, M. Liertzer, C. Deutsch, P. Klang, J. Schöberl, H. E. Tureci, G. Strasser, K. Unterrainer, and S. Rotter, “Reversing the pump dependence of a laser at an exceptional point,” *Nat. Comm.* **5** (2014).
- ⁹⁴Z. Lin, H. Ramezani, T. Eichelkraut, T. Kottos, H. Cao, and D. N. Christodoulides, “Unidirectional invisibility induced by \mathcal{PT} -symmetric periodic structures,” *Phys. Rev. Lett.* **106**, 213901 (2011).
- ⁹⁵I. Vorobeichik, M. Orenstein, and N. Moiseyev, “Intermediate-mode-assisted optical directional couplers via embedded periodic structure,” *IEEE J. Quant. Elect.* **34**, 1772–1781 (1998).
- ⁹⁶J. J. Wiersig, “Enhancing the sensitivity of frequency and energy splitting detection by using exceptional points: application to microcavity sensors

- for single-particle detection,” *Phys. Rev. Lett.* **112**, 203901 (2014).
- ⁹⁷J. D. Joannopoulos, S. G. Johnson, J. N. Winn, and R. D. Meade, *Photonic Crystals, Molding the Flow of Light* (Princeton University Press, 2008).
- ⁹⁸A. W. Snyder and J. Love, *Optical waveguide theory* (Springer Science and Business Media, 2012).
- ⁹⁹M. Skorobogatiy and J. Yang, *Fundamentals of photonic crystal guiding* (Cambridge University Press, 2009).
- ¹⁰⁰J. Hu and C. R. Menyuk, “Understanding leaky modes: slab waveguide revisited,” *Adv. Opt. Photonics* **1**, 58–106 (2009).
- ¹⁰¹N. Moiseyev, *Quantum Mechanics: From Fundamental Principles to Applications (in Hebrew)* (Y. L. Magnes, Hebrew University, 2015).
- ¹⁰²A. Taflöv, A. Oskooi, and S. G. Johnson, “Advances in ftdt computational electrodynamics: Photonics and nanotechnology,” p. 76, Readable online at <http://arxiv.org/ftp/arxiv/papers/1301/1301.5366.pdf> (2013).
- ¹⁰³O. Shemer, D. Brisker, and N. Moiseyev, “Optimal reflection-free complex absorbing potentials for quantum propagation of wave packets,” *Phys. Rev. A* **71**, 032716 (2005).
- ¹⁰⁴M. V. Berry, “Classical adiabatic angles and quantal adiabatic phase,” *J. Phys. A: Math. Gen.* **18**, 15 (1985).
- ¹⁰⁵S. Gasiorowicz, *Quantum physics* (John Wiley & Sons, 2007).
- ¹⁰⁶S. Y. Lee, J. W. Ryu, J. B. Shim, S. B. Lee, S. W. Kim, and K. An, “Divergent petermann factor of interacting resonances in a stadium-shaped microcavity,” *Phys. Rev. A* **78**, 015805 (2008).
- ¹⁰⁷P. T. Kristensen, C. Van Vlack, and S. Hughes, “Generalized effective mode volume for leaky optical cavities,” *Opt. Lett.* **37**, 1649–1651 (2012).
- ¹⁰⁸N. Marcuvitz, “Waveguide handbook,” p. 39 (Peter Peregrinus Ltd, 1951).
- ¹⁰⁹L. Novotny and C. Hafner, “Light propagation in a cylindrical waveguide with a complex, metallic, dielectric function,” *Phys. Rev. E* **50**, 4094 (1994).
- ¹¹⁰K. H. Chlereth and M. Tacke, “The complex propagation constant of multilayer waveguides: An algorithm for a personal computer,” *IEEE J. Quant. Elect.* **26**, 627–630 (1990).
- ¹¹¹E. Anemogiannis and E. N. Glytsis, “Multilayer waveguides: efficient numerical analysis of general structures,” *J. Light. Tech.* **10**, 1344–1351 (1992).
- ¹¹²I. Vorobeichik, U. Peskin, and N. Moiseyev, “Modal losses and design of modal irradiance patterns in an optical fiber by the complex scaled (t,t’) method,” *JOSA B* **12**, 1133–1141 (1995).
- ¹¹³G. Yoo, H.-S. Sim, and H. Schomerus, “Quantum noise and mode nonorthogonality in non-Hermitian \mathcal{PT} -symmetric optical resonators,” *Phys. Rev. A* **84**, 063833 (2011).
- ¹¹⁴R. G. Gordon, *Advances in Magnetic Resonance, Correlation functions for molecular motion*, edited by J. S. Waugh, Vol. 3 (Academic Press, 1968).
- ¹¹⁵L. Feng, Z. J. Wong, R.-M. Ma, Y. Wang, and X. Zhang, “Single-mode laser by parity-time symmetry breaking,” *Science* **346**, 972–975 (2014).
- ¹¹⁶B. Zhen, C. W. Hsu, Y. Igarashi, L. Lu, I. Kaminer, A. Pick, S.-L. Chua, J. D. Joannopoulos, and M. Soljacic, “Spawning rings of exceptional points out of Dirac cones,” *Nature* **525**, 354–358 (2015).